

INTERACTION OF A VOLUMETRIC METAMATERIAL STRUCTURE WITH AN ELECTRON BEAM

X. Lu, M. A. Shapiro, R. J. Temkin, MIT, Cambridge, MA 02139, USA

Abstract

A volumetric metallic metamaterial structure with a cubic unit cell is introduced. The unit cells can naturally fill all of space without additional substrates or waveguides. The structure can support a negative longitudinal electric mode that can couple to an electron beam. The dispersion characteristics of the unit cell are modeled by the effective medium theory with spatial dispersion. The theory also predicts the correct resonant frequencies of the emitted radiation excited by an electron beam traversing the structure. In the wakefield simulations, a backward radiation pattern is observed. The proposed metamaterial can be applied to beam diagnostics and wakefield acceleration.

INTRODUCTION

Metamaterials (MTMs) generally refer to subwavelength structures engineered to have exotic electromagnetic features. The resonator type [1] and the transmission line type [2] structures are developed as the negative refractive index MTMs for applications in electromagnetic cloaking, antenna design and microstrip lines, etc. However, the interaction of the MTMs with an electron beam is a new area of research and differs from the study of passive microwave devices where the planar MTM design is often adopted. The planar unit cells, like the split ring resonators, require supporting dielectric substrates, which will suffer from breakdown in the face of high power. Besides, electromagnetic fields are concentrated on the planar plates, so when an electron beam needs to be arranged in the structure, a reasonable spacing must be preserved between the beam and the planar structure, and the decreased field intensity at the beam location restricts the achievement of a large coupling impedance. These difficulties call for the design of a real 3D MTM unit cell. It should fill the space automatically, so we can study the fields in a bulk structure stimulated by the electron beam in a clean environment without the complexity arising from additional substrates or supporting parts.

In this paper, we will present the design of such a 3D MTM unit cell design. We will also introduce an analytical modeling technique, the effective medium theory with spatial dispersion. Radiation features and a possible application for wakefield acceleration will also be discussed.

DESIGN AND CHARACTERIZATION OF THE UNIT CELL

The unit cell is an all-metal coupled-cavity cubic crystal with beam holes and coupling slots. The structure design is shown in Fig. 1. The design frequency is 17 GHz, and the coupling slots through which the electromagnetic waves are coupled is about one tenth of the wavelength in size.

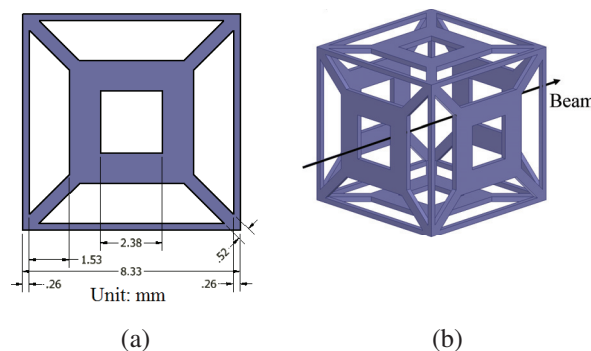


Figure 1: Unit cell geometry. (a) Face view. The thickness of each face is 0.26mm. (b) 3D view. In later sections we will put an electron beam on the axis.

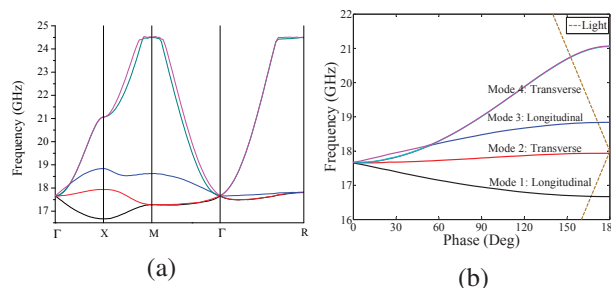


Figure 2: Brillouin diagram of the unit cell. (a) Different regions in the first Brillouin zone. (b) $\Gamma-X$ region dispersion showing intersection with the light line.

We use both numerical simulation and analytical modeling to study the dispersion relations of the unit cell.

Numerical Simulation

The HFSS Eigenmode Solver is used to calculate the dispersion curves in the first Brillouin zone, as shown in Fig. 2. The high symmetry points for a simple cubic lattice are $\Gamma(0, 0, 0)$, $X(\pi/p, 0, 0)$, $M(\pi/p, \pi/p, 0)$ and $R(\pi/p, \pi/p, \pi/p)$, where p is the period of the unit cell. We design the geometry to have a balanced structure with all the modes having the same cut-off frequency at the Γ point.

In the $\Gamma-X$ region, there are four modes. Among them, Mode 1 and Mode 3 are longitudinal, so they will couple strongly to an electron beam; Mode 2 and Mode 4 are transverse. The synchronized frequencies of the light line and the longitudinal modes are 16.7 GHz and 18.8 GHz, and the phase advance per cell is near 180° . Mode 1 can couple to the electron beam better than Mode 3, since in one unit cell Mode 1 has a field in the same direction, while Mode 3 has it in the opposite directions, as illustrated in Fig. 3.

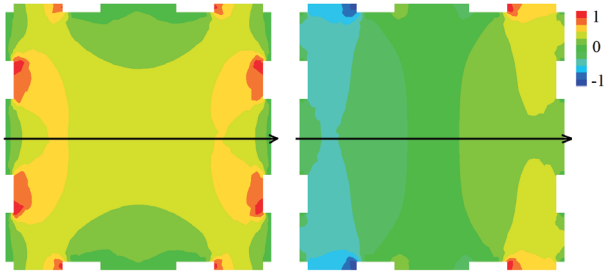


Figure 3: Field patterns of the longitudinal eigenmodes (Left: Mode 1, Right: Mode 3) in the $\Gamma - X$ region. Black arrows denote the path of an electron beam.

Effective Medium Theory with Spatial Dispersion

Below we demonstrate that the unit cell can be modeled with the effective medium theory with spatial dispersion. The effective medium theory aims to homogenize a periodic structure by retaining the electromagnetic characteristics. Spatial dispersion here is important because the electric field is not local due to the microstructure of the unit cell. So we decide the constitutive relation by

$$D_i(\omega, \mathbf{k}) = \sum_j \epsilon_{ij}(\omega, \mathbf{k}) E_j(\omega, \mathbf{k}), \quad (1)$$

where

$$E_i(\omega, \mathbf{k}) = \frac{1}{(2\pi)^4} \int dt \int d\mathbf{r} E_i(\mathbf{r}, t) e^{-i(\mathbf{k} \cdot \mathbf{r} - \omega t)}. \quad (2)$$

The permittivity tensor has the following form [3], [4]

$$\epsilon_{ii}(\omega, \mathbf{k}) = \epsilon_p(\omega) + \frac{\alpha_1 k_i^2 c^2 + \sum_{l \neq i} \alpha_2 k_l^2 c^2}{\omega^2 - \omega_p^2}, \quad (3)$$

$$\epsilon_{ij}(\omega, \mathbf{k}) = \frac{2\alpha_3 k_i k_j c^2}{\omega^2 - \omega_p^2}, \quad (i \neq j) \quad (4)$$

where $\epsilon_p = 1 - \omega_p^2/\omega^2$, and ω_p is decided by the cut-off frequency at the Γ point. We decide the remaining parameters α_1 , α_2 and α_3 from fitting the simulated dispersion curves to those analytically calculated from the dispersion equation in the medium

$$\det \left(\frac{\omega^2}{c^2} \epsilon_{ij} - k^2 \delta_{ij} + k_i k_j \right) = 0. \quad (5)$$

The fitting result is shown in Fig. 4, with the optimized parameters being $\alpha_1 = -0.021$, $\alpha_2 = 0$, $\alpha_3 = -0.0034$. In different regions of the Brillouin zone, the effect of the spatial dispersion differs. In the $\Gamma - X$ region, the dispersion curves are only decided by α_1 and α_2 , and it turns out $\alpha_2 = 0$ gives the best fit; while in the $\Gamma - M$ and the $\Gamma - R$ regions, all the three α parameters take effect.

INTERACTION WITH A RELATIVISTIC ELECTRON BEAM

Next we show that the effective medium model can characterize the interaction of an electron beam with a volumetric

3: Alternative Particle Sources and Acceleration Techniques

A16 - Advanced Concepts

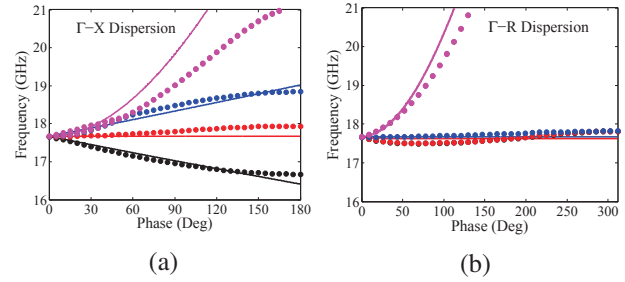


Figure 4: Comparison of the HFSS simulated dispersion curves (dotted lines) and analytically calculated curves with the effective medium theory (solid lines).

structure built with the proposed unit cell. Assume a point charge with a charge q moves with velocity \mathbf{v} in the $+x$ direction. We calculate $\mathbf{E}(\omega, \mathbf{k})$ from the Maxwell's Equations,

$$E_i(\omega, \mathbf{k}) = \sum_j i \frac{4\pi\omega}{c^2} A_{ij}^{-1} j_j(\omega, \mathbf{k}), \quad (6)$$

where the current

$$\begin{aligned} j_j(\omega, \mathbf{k}) &= \frac{qv_j}{(2\pi)^4} \int dt \int d\mathbf{r} \delta(\mathbf{r} - \mathbf{v}t) e^{-i(\mathbf{k} \cdot \mathbf{r} - \omega t)}, \\ &= \frac{qv_j}{(2\pi)^3} \delta(\omega - \mathbf{k} \cdot \mathbf{v}), \end{aligned} \quad (7)$$

and

$$A_{ij} = k^2 \delta_{ij} - k_i k_j - \frac{\omega^2}{c^2} \epsilon_{ij}. \quad (8)$$

Then the longitudinal electric field $E_x(\omega)$ is calculated by an integration over the whole \mathbf{k} space,

$$E_x(\omega) = -\frac{q\omega}{2\pi^2 c^2} \int dk_y \int dk_z \text{Im} A_{xx}^{-1} |_{k_x = \omega/v}. \quad (9)$$

We add a small loss term in the permittivity model by rewriting the denominators in the spatial dispersion terms from $\omega^2 - \omega_p^2$ to $\omega^2 - \omega_p^2 + i\Gamma\omega$, where $\Gamma \ll \omega$. Then after doing the integration numerically, we find two resonant peaks at 16.6 GHz and 19.1 GHz with an ultrarelativistic electron beam. The resonant peaks indicate a strong interaction with the beam, and we can test the result with the CST Wakefield Solver.

In the solver, we set up a short Gaussian bunch traveling at the speed of light on the central axis of 36 unit cells in a row. In the transverse directions, periodic boundary conditions are enforced. The wake impedance spectrum shows two resonant peaks at 16.4 GHz and 18.6 GHz. The agreement of numerical and analytical calculation is shown in Table 1, so the effective medium theory with spatial dispersion is a successful trial solution to predict the behavior of the MTM structure.

BACKWARD RADIATION PATTERN IN A BULK STRUCTURE

The 3D MTM structure is expected to generate the backward Cherenkov radiation, and we simulate this problem

Table 1: Comparison of Wave-beam Interaction Frequencies (Unit: GHz)

| | HFSS Eigenmode | Effective Medium | CST Wakefield |
|---------------|-------------------|---------------------|------------------|
| Mode 1 | 16.7 | 16.6 | 16.4 |
| Mode 3 | 18.8 | 19.1 | 18.6 |

with the CST Wakefield Solver. An electron bunch travels in the $+x$ direction through the central axis of a bulk structure (Fig. 5(a)) with 10, 7 and 7 unit cells in the x , y , and z directions, respectively. The structure rests in vacuum with open boundaries all around. Figure 5 shows the radiated longitudinal E_x field on the middle cutting plane in (c) and on the cross section in (d). Compared with the radiation pattern in a structure of the same geometry but filled with an artificial $\epsilon = 1.5$ dielectric as shown in Fig. 5(b), the MTM structure makes the electromagnetic energy travel backwards and leaves the major part of the energy in the vacuum region on the beam entrance end. From the cross section pattern in (d), we find the wave fronts are backward traveling cones.

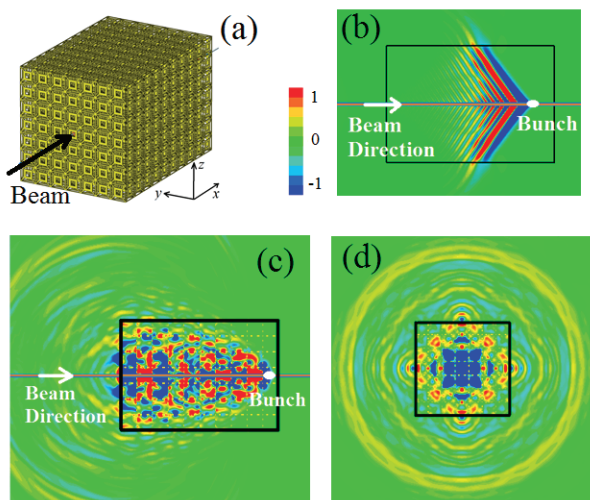


Figure 5: Backward Radiation Patterns. (a) Geometry of the bulk structure. (b) Longitudinal E field (E_x) on $y = 0$ middle cutting plane in a bulk made of a dielectric with $\epsilon = 1.5$. (c) E_x on $y = 0$ plane in the MTM. (d) E_x on the cross section ($x = \text{constant}$) in the MTM.

APPLICATION IN WAKEFIELD ACCELERATION

The backward propagating feature in the MTM structure can help build up the wakefields, and this mechanism can be applied to wakefield acceleration. We modify the unit cell from the 6-face cubic to 2 faces supported by 4 rods, and put a row of them into a waveguide, as shown in Fig. 6(a). In the CST Particle-In-Cell Solver, a driving bunch of 40 nC with an initial energy of 6 MeV is injected on axis, and a witness bunch of 1 pC follows it to be accelerated. The phase

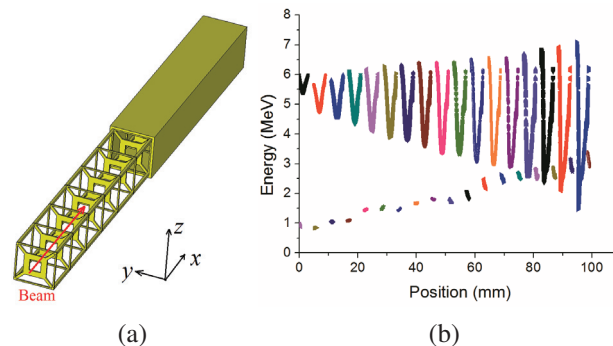


Figure 6: (a) Structure for wakefield acceleration. (b) Phase space evolution of the drive bunch (top) and the witness bunch (bottom). The witness bunch is injected into the structure 30 mm after the drive bunch.

space evolution of the two bunches is shown in Fig. 6(b). An average accelerating gradient of 22 MeV/m is achieved.

CONCLUSION

In conclusion, we have shown that the unit cell as designed can build a real 3D MTM. The negative dispersion mode is the fundamental mode, and it has a longitudinal electric field. Theoretically we have proved that a homogeneity approximation with spatial dispersion is good to describe the dispersion characteristics. When interacting with the relativistic electron beam, the MTM structure shows a backward radiation pattern, which can be applied to beam diagnostics and wakefield acceleration. Study of this structure can be useful for MTM-based vacuum electron devices.

ACKNOWLEDGMENT

This research was supported by the U.S. Department of Energy, Office of Science, Office of High Energy Physics under Award Number DE-SC0010075 and the Air Force Office of Scientific Research under MURI Grant Number FA 550-12-1-0489.

REFERENCES

- [1] R. Marqués, F. Martín, and M. Sorolla, *Metamaterials with Negative Parameters: Theory, Design and Microwave Applications*, (John Wiley & Sons, 2011).
- [2] C. Caloz and T. Itoh, *Electromagnetic Metamaterials: Transmission Line Theory and Microwave Applications*, (John Wiley & Sons, 2005).
- [3] V. M. Agranovich and V. L. Ginzburg, *Crystal Optics with Spatial Dispersion, and Excitons*, (Springer, 1984).
- [4] M. A. Shapiro et al., *Opt. Lett.* 31, 2051 (2006).